Biosensors and Bioelectronics 145 (2019) 111661

Contents lists available at ScienceDirect

Biosensors and Bioelectronics

journal homepage: www.elsevier.com/locate/bios

The use of a double-layer platinum black-conducting polymer coating for improvement of neural recording and mitigation of photoelectric artifact

Long-Chun Wang[a], Ming-Hao Wang[a], Chao-Fan Ge[b,c], Bo-Wen Ji[a], Zhe-Jun Guo[a], Xiao-Lin Wang[a], Bin Yang[a], Cheng-Yu Li[b,c], Jing-Quan Liu[a,*]

[a] National Key Laboratory of Science and Technology on Micro/Nano Fabrication Laboratory, Key Laboratory for Thin Film and Microfabrication of the Ministry of Education, Collaborative Innovation Center of IFSA, Department of Micro/Nano-electronics, Shanghai Jiao Tong University, Shanghai, 200240, PR China
[b] Institute of Neuroscience and Key Laboratory of Primate Neurobiology, Shanghai Institutes for Biological Sciences, Chinese Academy of Sciences, Shanghai, 200031, PR China
[c] University of Chinese Academy of Sciences, Peking, PR China

ARTICLE INFO

Keywords:
Optogenetics stimulation
Photoelectric artifact
Platinum black
Conducting polymer
Neural recording

ABSTRACT

The impedance of electrode and photostimulation artifacts (short-duration and high-amplitude spikes) are still hindering the employment of silicon-based neural probe in optogenetics. A fiber-based optrode modified with a double-layer platinum black-poly (3,4ethylenedioxythiophene) PEDOT/poly (4-styrenesulfonate) PSS (Pt-PP) coating has been developed for improvement of neural recording quality and mitigation of photoelectric artifact simultaneously. The Pt-PP coating was made by layer-by-layer electrochemical deposition followed by the ultrasonication and Cyclic Voltammetry (CV) scanning to verify its mechanical and electrochemical stability. Both *in-vitro* and *in-vivo* experiments demonstrated that Pt-PP coated optrode had outstanding recording performance (high signal-to-noise ratio about 9.64) and low photoelectric amplitude (850 μV). The artifact recovery time of Pt-PP coated optrode (0.3 ms) after photostimulation was significantly decreased when compared to platinum black (6 ms) or PEDOT/PSS (0.7 ms) coated one which has potential to retain high-quality neural signals in animal experiments. At last, the optogenetics experiments revealed the capability of Pt-PP coated optrode to record the change in neural spike rate with certain spatial resolution and shorter artifact recovery time. These results suggest that Pt-PP coating has great potential for neural electrodes in the application of neuroscience.

1. Introduction

Optogenetics has emerged as an effective tool for neural scientists to understand the architecture and function of neural system circuits in recent years, which is a new technology to achieve cell-type specific neuromodulation with millisecond-scale temporal precision (Goncalves et al., 2017). The employment of light activation or inhibition for evaluating neural system network dynamic requires synchronous application of neural recording techniques and external network modulation (Li et al., 2018; Wu et al., 2015). Combining optogenetics and electrophysiological recordings is the tendency to achieve the ultimate goal of catalyzing new treatments for brain disorders and diseases, such as dysfunctional parkinsonian motor control (Kravitz et al., 2010; Vazey and Aston-Jones, 2013), blindness (Henriksen et al., 2014) and depression (Lobo et al., 2012). The silicon-based neural probes are turning into welcome recording tools in neural science due to the high density, customization of recording sites and the repeatability low unit costs meet the demand of batch fabrication schemes (Fekete, 2015).

So far, two specific challenges arise when combining optical stimulation and silicon-based neural probe recordings *in-vivo*. The first one is the direct laser beam striking metal which can induce electrical artifacts with various short duration and high amplitude during electrophysiological recordings (Cardin et al., 2009; Han et al., 2009; Khurram and Seymour, 2013). These artifacts whose emerged causes ranging from possible photoelectric effects to temperature-dependent effects on electrode conduction properties. It can contaminate biosignals and preclude useful data from being acquired (Cardin et al., 2010). The interface material and impedance level of electrode are relevant to the artifact (Khurram and Seymour, 2013). Glass-based optrodes have been reported to mitigate the artifact (Canales et al., 2015; Dufour et al., 2013; LeChasseur et al., 2011). However, limited by the quantity of the recording sites, high spatial and temporal resolution is unachievable for glass-based optrodes. The second challenge is the electrode sites of silicon-based neural probe downsized to microscale

* Corresponding author.
E-mail address: jqliu@sjtu.edu.cn (J.-Q. Liu).

https://doi.org/10.1016/j.bios.2019.111661
Received 6 May 2019; Received in revised form 14 August 2019; Accepted 27 August 2019
Available online 29 August 2019
0956-5663/

with a diameter ranging from 7.5 μm to 20 μm, whose primordial thin-film Aurum (Au), Platinum (Pt), and Iridium (Ir) would all produce significant noise without additional steps to increase surface roughness or decrease impedance (Seymour et al., 2017). Modification of the electrodes is an effective way to lower the impedance and recording noise (Luo et al., 2019; Zeng et al., 2019). As is known, electroplated Au (Du et al., 2009), platinum black (Rui et al., 2012), reactive sputtering of tin (Weiland et al., 2002), and sputtered iridium oxide (Ji et al., 2018; Negi et al., 2010) are common modification methods, which show significantly improvement of electrode performance. Nonetheless, the surface photoelectric effect in thin metal overlayers has been one of the most long-standing problems in metal physics (Petersen and Hagström, 1978; Wallden, 1985) which give rise to intense electric artifact to vitiate useful neural signal. Therefore, it is urgent to develop a low recording noise electrode-tissue interface for signal quality improvement without intense photoelectric artifact.

Over the last decade, inherently conducting polymers, particularly poly (3, 4-ethylenedioxythiophene) doped with poly (4-styrenesulfonate) (PEDOT/PSS) has been studied in neural probe and prosthetic research as a means of improving the electrode-tissue interface (Cogan, 2008; Ludwig et al., 2006). It can greatly ameliorate the electrode-tissue communication by reducing impedance and increasing charge injection limit dramatically (Kovalenko et al., 2010). Compared with the metal, conductivity in polymer materials arises from the presence of conjugated double bonds along the backbone of an insulative structure (Green et al., 2008) rather than the loosely held electrons which may absorb energy from photons. Meanwhile, it is hard to manufacture photosensitive polymeric materials for the lack of special chromophore groups in them to absorb a photon (Aleksandrova, 2007), which explain the poor photosensitivity performance of polymeric materials. Hence, the PEDOT/PSS coating is able to mitigate photoelectric artifact to some extent. However, challenges in conducting polymers include poor electroactive stability and mechanical properties which limit its application in long-term implantation *in-vivo* (Green et al., 2008; Kozai et al., 2016; Zhang and Zhao, 2012).

Taking the performance of noble metals and conducting polymers into account, in this study, we report a double-layer platinum black-PEDOT/PSS (Pt-PP) coating for the application of neural recording combined with optogenetics. The double-layer Pt-PP coating was obtained by electrochemical layer-by-layer deposition. A thin layer of platinum black was electroplated by pulse current under ultrasonication firstly to roughen the surface of Au electrode, and then the galvanostatic method was applied to electroplate another layer of PEDOT/PSS coating. The performance of recording stability and improvement of signal to noise ratio, especially the mitigation of photoelectric artifact by Pt-PP coating were verified. To the best of our knowledge, electrochemical modification of electrode to alleviate photoelectric artifact during optogenetics has rarely been reported.

2. Materials and methods

2.1. Regents and materials

All solutions, if not specified, were prepared in deionized water (DI). PSS and EDOT were purchased from Sigma Aldrich Chemicals Co. (USA). Chloroplatinic acid, lead acetate and phosphate buffered saline (PBS, pH7.4) were purchased from Sinopharm Chemical Reagent Co.,Ltd (China). ACF (AC-7813KM) was purchased from Hitachi chemical Co.,Ltd (USA). SOI wafers were purchased from RDMICRO Co.,Ltd (China).

2.2. Microelectrodes fabrication

Figure S1 showed the fabrication process of the silicon-based microelectrodes. A P-type, silicon-on-insulator (SOI) was chosen as substrate. The thickness of the silicon device layer, the buried oxide layer and the handle layer of the SOI were 30 μm, 2 μm, and 475 μm respectively. A detailed description of the fabrication process is shown in our previous work (Wang et al., 2018b). The microelectrode has four shafts with a dimension of 8 mm length, 100 μm width and 30 μm thickness, 32-channel distribute over 4 shanks uniformly and every four recording sites with area of 121 μm^2 merge into a tetrode (Fig. S2).

2.3. Construction of the fiber-based optrode

To obtain optrode that enable both electrophysiology recording and optical stimulation of local cluster of neurons, the micro-scale optical fiber and home-made silicon microelectrodes was assembled together. A flexibility Polyimide (PI) cable joint the microelectrodes and Printed circuit board (PCB) together (Fig. S3) with the aid of anisotropic conductive film (ACF). Firstly, the probe was placed on the glass slide, a layer of ACF was stuck on the surface of bonding pads, then the first ACF lamination was operated at 140 °C, and 0.14 MPa for 3 s after alignment of bonding pads with the heat head of the ACF attachment machine. After the releasing film of ACF was peeled off, placed the PI cable on the surface of the ACF coated bonding pads and a precise alignment was conducted under a microscope. Then the final bonding was operated at 240 °C, and 0.18 MPa for 18 s after alignment of PI cable with the heat head of the ACF attachment machine. The ACF bonding process of the PCB with the PI cable was similar to that of the probe with the PI cable.

After the microelectrode was packaged, the integration of optical fiber to microelectrode started with the treatment of optical fiber. A diamond knife was used to incise fiber so as to obtain a smooth output facet. After that, the probe was mounted on a glass slide. The optical fiber was placed on the shank of silicon probe with the aid of micromanipulators under microscopic view. When the fiber was in right place where fiber output facet should be 100 μm away from the recording sites (Royer et al., 2010). A needle tubing was used to infuse the epoxy around the fiber at the root of probe. The glass slide was placed for 15 min in an oven maintained at 70 °Cfor immobilization of the epoxy.

2.4. Preparation of electrolyte and electrochemical deposition

The electrolytes for platinum black deposition included the following: Firstly, 1.5 g Chloroplatinic acid (3%) was added to 50 ml deionized water and stirred for 10 min to dissolve, then 5 mg lead acetate was added.

The electrolytes for PEDOT/PSS deposition consisted of the following: Firstly, 250 mg PSS was added to 50 ml deionized water, then ultrasonic treatment was made for 5 min and stirred for 10 min to dissolve the components. Lastly, 0.01 M EDOT was added, and the solution was stirred for 1 h to obtain the electrolyte solution.

The best modification parameters were identified by measuring the electrochemical impedance spectrum (EIS) of modified electrode with different deposition cycles (platinum black) and deposition time (PEDOT/PSS). After multiple comparison experiments (Fig. S4), the best modification parameters were obtained as follows: the electrochemical deposition of platinum black was carried out under ultrasonication. Repetitive current pulses (duty ratio of 5 ms: 500 ms, peak current density of 4.5 mA/cm^2, cycles of 200) was generated with electrochemical workstation (CHI660C,CH instrument) by using a gold rod as the reference and the counter electrode. Then the constant current (current density of 0.2 mA/cm^2, time of 10 min) was applied to electroplate PEDOT/PSS in a three-electrode cell with a Pt foil as counter electrode and saturated calomel electrode (SCE) as reference electrode. Meanwhile, two optrodes were modified with single layer platinum black and PEDOT/PSS respectively. The modification parameters are the same with double Pt-PP coating to investigate the difference of optrodes modified with three coatings.

2.5. In-vitro characterization

The electrochemical properties of the microelectrodes were closely related to the performance of electrophysiological signal recording. Both the cyclic voltammetry (CV) and electrochemical impedance spectroscopy (EIS) test were carried out by using Autolab (PGSTAT204, Switzerland) with a Pt foil as counter electrode and SCE as reference electrode in phosphate-buffered saline (PBS, 0.1M, pH 7.4). Applied frequency of EIS ranged from 0.1 Hz to 100 kHz at an amplitude of 10 mV. The potential range of CV scan was from −0.6 V to 0.8 V at a scanning rate of 0.1 V/s.

The interference of photoelectric artifact to microelectrodes seriously depended on the amplitude and the recovery time. Light-induced artifacts show an onset ramp that continues for the duration of a stimulus which able to submerge biosignals and preclude useful data from being acquired during stimulation (Cardin et al., 2010). Photoelectric artifact and background noise tests were performed in a shielding box. The fiber-based optrode was fixed at a 3D micromanipulator and immersed in PBS solution (0.1M, pH 7.4) with an optical fiber connect to 473 nm laser source (BL473T3-100FC, Laser& Optical Century) which transmitted blue light to the tip of microelectrodes. The signal acquisition system was composed of an RHD2000 Evaluation System (Intan Technology, LA, CA) connected to a computer with sampling frequency 20 kHz and band-pass filtered from 250 to 8000 Hz. A series of blue light with frequency of 10 Hz, duration of 50 ms, optical power of 0.03, 0.3, 1, 2, 6, 9, 12 mW were used to investigate photoelectric artifact. The background noise and photoelectric artifact in PBS solution were recorded without or with light radiation respectively.

The largest component of background noise *in-vitro* is thermal noise which can be defined as follows:

$$V_{noise} = \sqrt{4kTZ\Delta F} \quad (1)$$

where k is Boltzman's constant, T is the temperature, △F is the frequency band of interest and Z is the impedance at the frequency band of interest (Ludwig et al., 2006). Therefore, the recorded noise *in-vitro* varies with the impedance of the electrode when T and △F are certain values. The root-mean-square (RMS) noise voltage for each recording with electrodes in PBS solution was calculated by Matlab and the recording performance of electrode was characterized. The negative amplitude of photoelectric artifact is defined as “the generated negative photovoltage amplitude at the time when light is on” and the recovery time is defined as “interval from the generation of photovoltage to the amplitude decreasing to baseline”.

2.6. In-vivo experiment

In-vivo experiment was performed on male adult mice infected with Thy1-ChR2-YFP (Jackson Labs 07615). All animal studies and experimental procedures were approved by the Animal Care and Use Committee of the Institute of Neuroscience, Chinese Academy of Sciences, Shanghai, China. The isoflurane was used to narcotize mice before surgery, then the skull was exposed after scalp and soft tissue were removed and rinsed with 3% hydrogen peroxide solution and filtered artificial cerebrospinal fluid (ACSF) with cotton applicators. Next, a layer of tissue adhesive (Kwik-Sil) was daubed on the surface of the skull and then a steel plate was placed which was fixed by dental cement. After that, the mice were settled at the stereotaxic frame by the steel plate and craniotomies of ~2 mm in diameter were operated above the Ventral tegmental area (VTA). Finally, the fiber-based optrodes were implanted to the working sites where 4.2 mm below the cortical surface and the PCB was fixed on the metal plate by dental cement for the chronic implantation.

In chronic animals recording experiments, the male adult mice were undergone normal feeding for four weeks after optrodes implantation. The recording was carried out to testify the electrical recording and prolonged implantation stability of optrodes modified with different coatings. PEDOT/PSS coated optrode was not carried *in-vivo* experiment for its poor electroactive stability, mechanical stability in long-term chronic experiments (Green et al., 2008; Kozai et al., 2016; Zhang and Zhao, 2012).

A Multi-channel Neural Acquisition Processor (Plexon Inc, Dallas, TX) was used to record neural signals which were amplified and band-pass filtered. The neural signals were sampled at 40 kHz and band-pass filtered from 250 to 8000 Hz, while local field potentials were band-pass filtered from 0.5 to 250 Hz. Animals were settled in an electrically shielded box during recording. *In-vivo* optogenetic experiments, a series of blue light with power of 2 mW (corresponding to 255 mW/mm^2), frequency of 1, 5, 10, 20, 40 Hz (5 ms duration, 10 pulses for each frequency) were applied simultaneously with signal recording.

OfflineSorter was applied to perform Offline spike detection. Raw signals were filtered in 250–8000 Hz. Typically negative three times of standard deviation of recorded signals were set as thresholds for detecting spike events and deflections lower than the threshold were marked as putative spike events. The maximal peak-to-peak amplitude of each cluster was identified as signal amplitude. The data used for RMS noise voltage calculation should be pure noise data after all spike waveform segments 250 μs before and 750 μs after the threshold crossings have been removed, then the Matlab was used to calculate the RMS noise (Wang et al., 2018a). So, the signal-to-noise ratio (SNR) for a given cluster was defined as follows:

$$\text{SNR} = \text{Signal Amplitude} / (2 \times \text{Averaged RMS Noise Voltage}) \quad (2)$$

3. Results and discussion

3.1. Construction and modification of the fiber-based optrode

The schematic diagram of the construction and modification of the fiber-based optrode is shown in Fig. 1a. The package of silicon-based microelectrode was made by the ACF bonding to rear-end PCB, and then a single-mode optical fiber was fixed at root of the probe by epoxy. Fig. 1b shows the microelectrode used throughout this work compared with a coin. It is tiny enough only about 0.035g which has little effect on the normal life of mice in long-term implantation. The partition view of ACF bonding was shown in Fig. 1d. The trenches encircled bonding pad have a depth about 32 μm and a dimension of 150 μm × 400 μm which is large enough to satisfy the area of ACF bonding (Wang et al., 2018a). The conductive particles were only released from Au bonding pads to realize unidirectional conduction (Fig. S5). Fig. 1e shows the optical fiber with smooth outlet facet is assembled into the center of four shanks. The outlet of fiber should be about 100 μm away from the nearest recording site to ensure the light-evoked neural activity well recorded.

The fiber-based optrode was modified with double-layer Pt-PP coating to improve the recording performance as illustrated in Fig. 1c. A thin layer of platinum black (black circle) was electroplated via pulse current under ultrasonication to roughen the surface of Au electrode, then the galvanostatic was applied to electroplate another layer of PEDOT/PSS (red circle) on platinum black with rough and porous surface. The reproducibility of this modification method was also verified (Fig. S6). In brief, the batch fabrication technique, construction and modification method are important to ensure the consistency of the fiber-based optrode.

3.2. Recording performance characterization

The recording performance of Pt-PP coated optrode was firstly verified by electrochemical testing. The measurement of charge storage capacity (CSC) using CV is a common way of electrode material characterizing. Fig. 2a illustrates that the CV curve of Pt-PP coated optrode

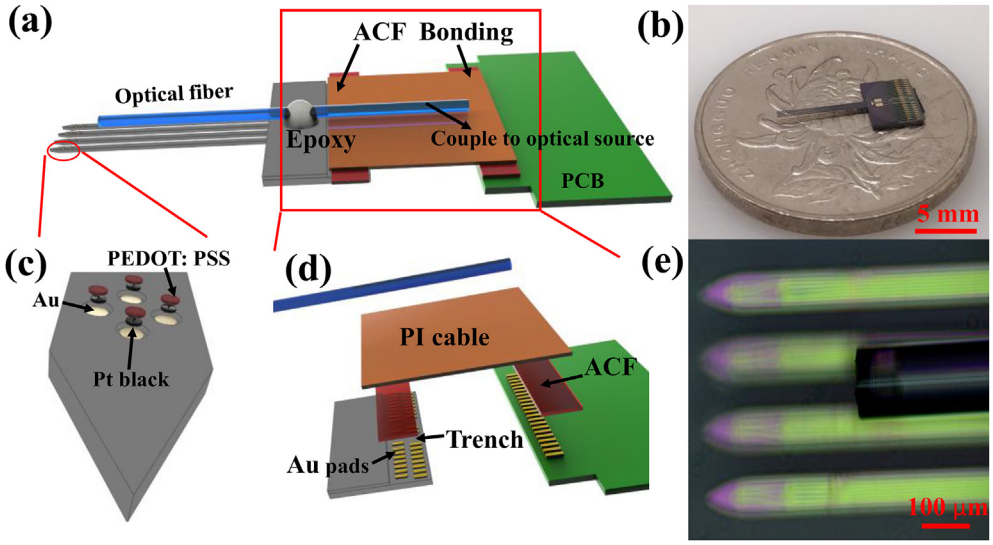

Fig. 1. The construction of the Pt-PP coated optrode. (a)The assembly of the fiber-based microelectrode. (b) A homemade microelectrode compared with a coin. (c) The schematic diagram of the Pt-PP coating patterning at the surface of Au electrode via layer-by-layer deposition. (d) The partition view of the ACF bonding structure. (e) The micrograph of an optical fiber fixed at the tip of the probe, and the outlet of fiber is about 100 μm away from recording sites.

has a larger enclosed area than PEDOT/PSS coated optrode and thence holds a larger CSC, which meant excellent charge injection capacity. While the reductive peak at about −0.3 V of platinum black is attribute to pseudocapacitance property (Merrill et al., 2005). Impedance at 1 kHz is important for neural recording electrodes for the pulse width of an action potential is approximately 1 ms (Khurram and Seymour, 2013). From Fig. 2b and c, the EIS curve shows Pt-PP coated optrode has two orders lower magnitude of impedance than bare Au in all frequency ranges and the phase angle of Pt-PP coated optrode is similar to PEDOT/PSS at low frequency (1–100 Hz) and similar to platinum black at high frequency (10^3–10^5 Hz). Meanwhile, the impedance of Pt-PP coating decreases to 47 kΩ lower than PEDOT/PSS (91 kΩ) and platinum black (58 kΩ) at 1 kHz which indicate good electrochemical performance of Pt-PP coating (Fig. 2d, n = 3). The inset in Fig. 2d shows the electroplating consistency of Pt-PP coating on the bare Au electrodes.

The background noises in PBS solution recorded by signal acquisition system of different modification electrodes are shown in Fig. 2e.It shows obvious noise burrs in Au electrodes and the RMS noise was 321 μV. The noise burrs disappeared and noise baseline dropped rapidly after modification. The RMS noises of PEDOT/PSS, platinum black, Pt-PP coating are 111 μV, 92 μV and 59 μV respectively, which is in accordance with impedance performance showed in Fig. 2b. In a word, compared to PEDOT/PSS and platinum black, the Pt-PP coated optrode shows outstanding performance in recording ability.

3.3. Photoelectric artifact characterization

The photoelectric artifact tests were carried out in a shielding box to isolate electromagnetic interference in the air as shown in Fig. 3a. The waveforms of photoelectric artifact recorded in PBS solution are illustrated in Fig. 3b, c, d. As the optical power increases, the artifact amplitude induced by photons augments as well, but the trend of augment and waveform are different which depends on different modified materials. Meanwhile, the amplitude of photoelectric artifact of Pt-PP coated optrode falls to almost 0 mV at optical power of 0.03 mW (corresponding to 3.82 mW/mm^2) which is enough to activate opsin-expressed neurons (Stark et al., 2012). The histograms in Fig. 3e show the Pt-PP coated optrode obtains the lowest negative artifact amplitude which attribute to the direct light irradiation on polymeric material (PEDOT/PSS), and the lower impedance spectrum of Pt-PP coated optrode accounted for the lower artifact amplitude than PEDOT/PSS coated one, because the impedance level of electrode is positive related to the artifact (Khurram and Seymour, 2013). Compared to platinum black, the negative artifact amplitudes of Pt-PP and PEDOT/PSS coated optrodes decrease by 58.5 ± 0.9% (n = 3) and 42.6 ± 1% (n = 3) respectively at optical power of 2 mW. The recovery time marked in artifact waveforms of different coatings is illustrated in Fig. 3f. Pt-PP coated optrode holds the shortest recovery time (0.3 ms) which is able to greatly retain useful neural signal *in-vivo*.

3.4. Stability experiment

The mechanical agitation and CV scanning were applied to measure the mechanical and electrochemical stability of Pt-PP coating on electrodes. The detailed description of test is shown in our previous work (Wang et al., 2018b). Firstly, a CV scanning was performed from −0.6 V to 0.8 V in PBS solution with a scanning rate of 1 V/s and scanning cycles of 10000 to research the electrochemical cycling stability. Then, the optrode was inserted into brain model made of agarose shown in the inset of Fig. 4a, an ultrasonic bath was applied with a power of 50 W to simulate the micromotion of brain tissue. The impedance spectrum error diagram of electrode before and after CV scanning and sonication treatment are illustrated in Fig. 4a. The impedance at 1 kHz increases by 9.5 ± 0.7% (n = 3) and CSC value decreases by 4.2 ± 1.8% (n = 3) after 10000 CV cycles. On this basis, increment of impedance 7.8 ± 1.2% (n = 3) at 1 kHz and decrement of CSC 3.9 ± 1.3% (n = 3) are obtained after 100 min sonication (Fig. 4b). The SEM images of bare Au and platinum black coated electrode are shown in Fig. 4c and d. Bare Au electrode displays a smooth surface while electrode modified with platinum black obtains rough and porous surface (inset in Fig. 4d) which can enhance the mechanical strength of later PEDOT/PSS electroplating. The CV scanning and ultrasonication experiments confirm that Pt-PP coated optrodes are qualified to execute long term recording *in-vivo*.

3.5. In-vivo neural recording and optogenetics experiment

The outstanding recording performance of Pt-PP optrode is shown in Fig. 5. As illustrated in Fig. 5a, b,the spikes are more apparent in Pt-PP coated optrode than platinum black coated one on account of lower background noise, and this may give the credit to the outstanding electrochemical performance of Pt-PP coating described in section 3.2. The corresponding SNR of the Pt-PP and platinum black coated electrodes are 9.64 and 7.14 respectively. Fig. 5c shows the representative neuronal spikes recorded from Pt-PP coated optrode with average peak-to-peak amplitude of 220 μV and corresponding firing rate of 7 Hz (Fig. 5d). The principal component analysis of the recorded spikes is

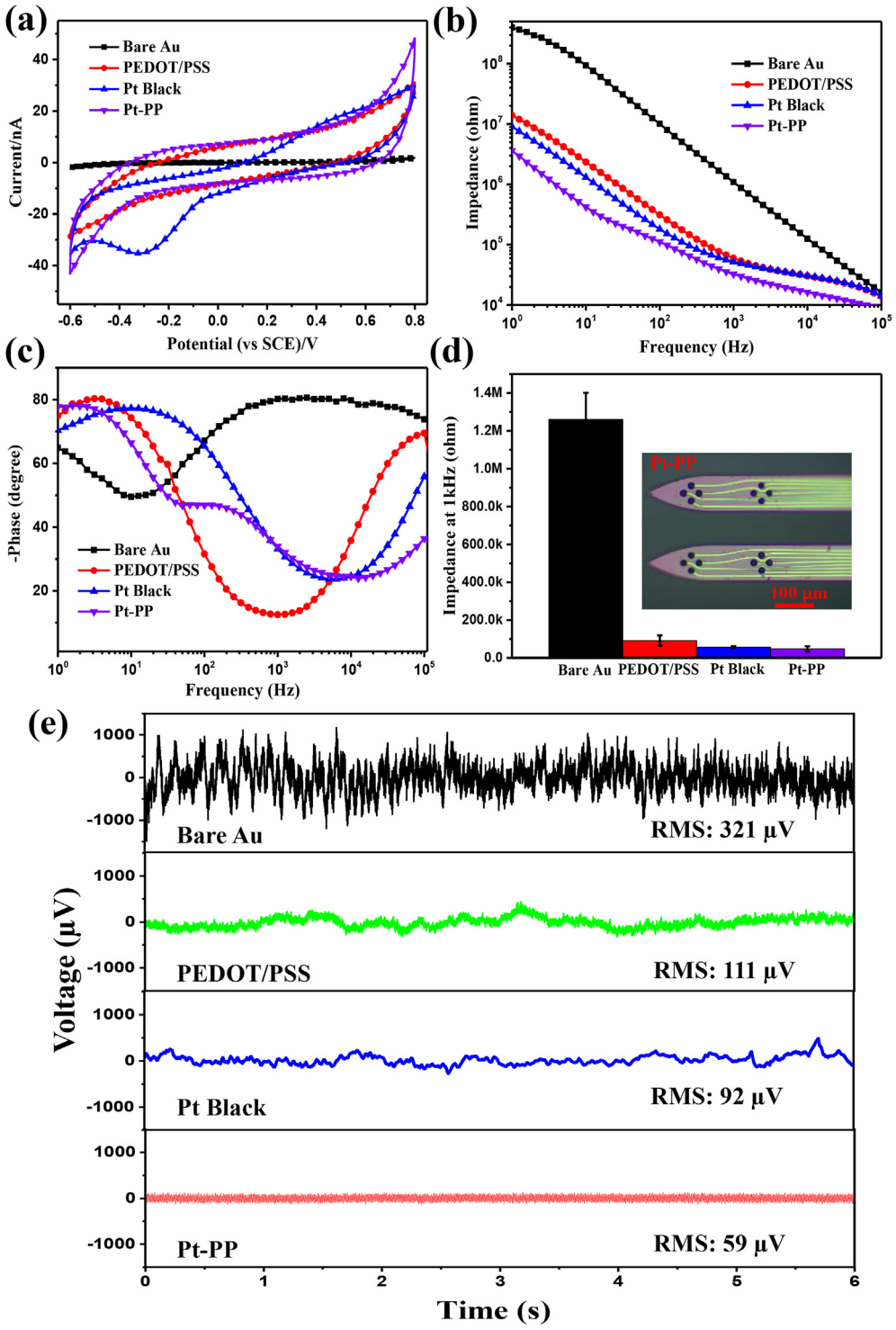

Fig. 2. The electrochemical characterization of Bare Au, PEDOT/PSS, PtBlack, Pt-PP coated optrode. (a) CV and (b, c) EIS diagrams of Bare Au, PEDOT/PSS, PtBlack, Pt-PP coated optrode. (d) The histograms show the impedance at 1 kHz of Pt-PP coated optrode lower than PEDOT/PSS, PtBlack coated optrode, (the inset shows the micrograph of Pt-PP coating modified microelectrodes). (e) The background noise of electrode modified with different coatings recorded in PBS solution with a sampling rete of 20 kHz, and Pt-PP coated electrode shows the lowest RMS noise of 59 μV.

shown in Fig. 5e, and the 3D cluster of each spike indicates little otherness.

Optogenetics experiments were carried out by applying a train of laser pulses with power of 2 mW at the outlet of the fiber in VTA and recording neural signal simultaneously (Fig. 6a). Fig. 6b shows the 16 channels spontaneous action potentials recorded from Pt-PP coated optrode during three laser pulse trains. Fig. 6c and d shows the recorded signal during a laser pulse train and the negative artifact amplitudes for platinum black and Pt-PP coated optrodes are about 2300 ± 100 μV (n = 3) and 850 ± 100 μV(n = 3) respectively. The frequency change has little effect on the artifact amplitude. On the other hand, the enlargement of one artifact waveform (Fig. 6e and f) from Fig. 6c and d at frequency of 10 Hz illustrates the recovery time (1.11 ms) of Pt-PP coated optrode is lower than platinum black coated

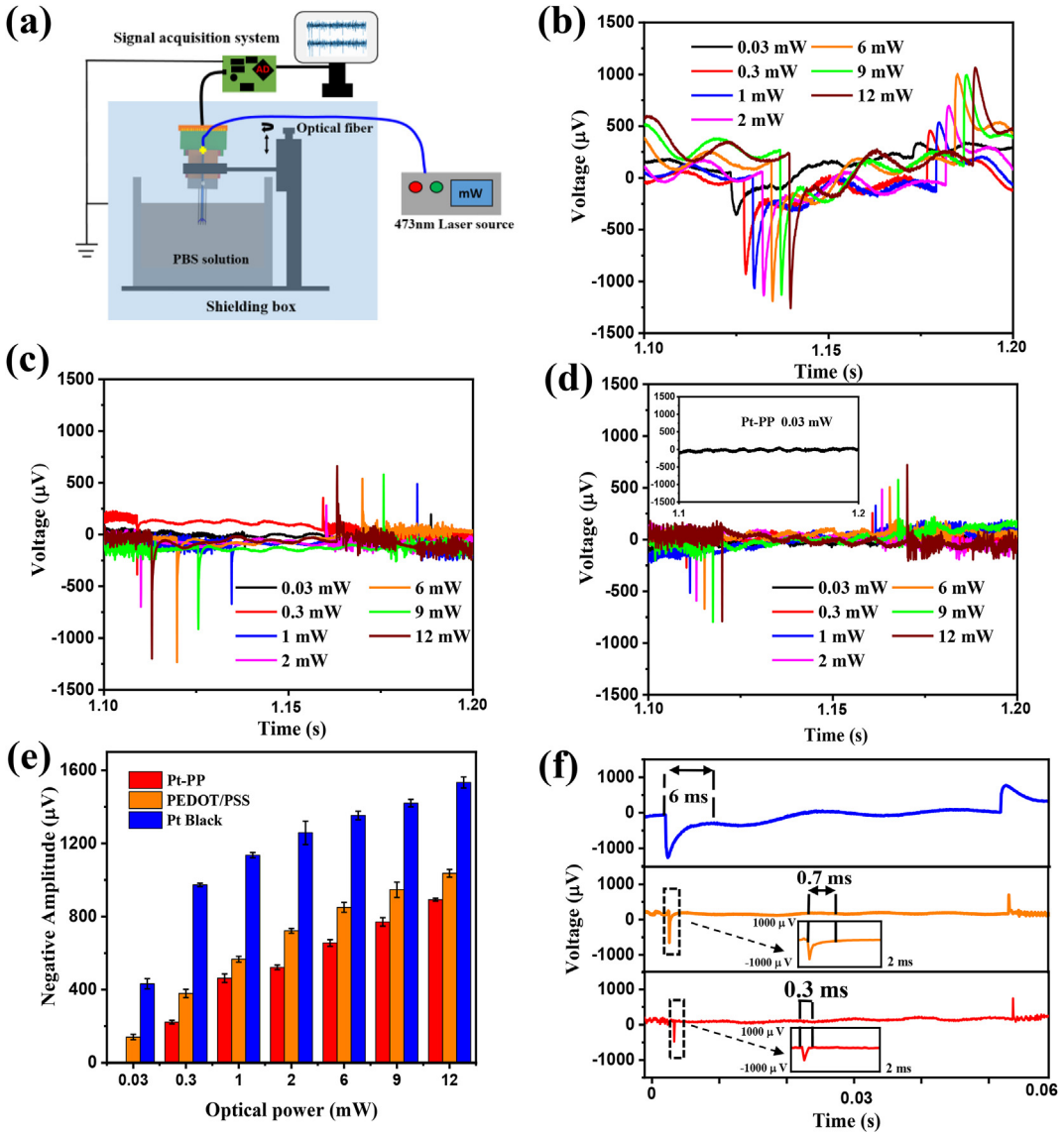

Fig. 3. The results of photoelectric artifact characterization *in-vitro*. (a) The schematic diagram of background noise and photoelectric artifact tests. The photoelectric artifact of electrodes modified with different coatings at different optical power. (b) Platinum black, (c) PEDOT/PSS, (d) Pt-PP (Inset shows the recorded signal of Pt-PP modified optrode at optical power of 0.03 mW). (e) The histograms of negative amplitude comparison at different optical power. (f) The waveforms in one photostimulation period of the platinum black, PEDOT/PSS, and Pt-PP coating at optical power of 2 mW.

one (2.45 ms). The laser pulses (duration of 5 ms, frequency of 10 Hz) are competent for activating the ChR2-expressed neurons in VTA(Eshel et al., 2015). The neural spiking events can be recorded obviously during light pulse stimulation (Fig. S10) owing to the shorter recovery time and lower amplitude of Pt-PP coated optrode can greatly retain useful signal. The difference of the recovery time between *in-vivo* and *in-vitro* tests at power of 2 mW may attribute to the refractive index of brain tissue. Fig. 6g illustrates the raster pattern and recorded signal in electrode 1 (Fig. 6i) of Pt-PP coated optrode before and after a train of laser pulses. Each vertical line in raster pattern represents a spiking event, the black line represents non responsive spiking event while the blue line represents light modulation spiking event whose firing rate is modulated by light pulse. Neural waveform 1 and waveform 2 are recorded in different electrodes and illustrated in Fig. 6i, the waveform and trend of firing rate in Fig. 6h are almost the same which indicate the two waveforms are fired by the same neuron whose position is closer to electrode1. Meanwhile, both of the firing rates increased significantly when the laser was turned on and return to normal after the laser was turned off, which demonstrated the neuron was modulated by blue light. The results reveal that Pt-PP coated optrode is competent for long-term optogenetics application.

4. Conclusions

In conclusion, we have developed a fiber-based optrode modified with a double-layer Pt-PP coating for improvement of neural recording performance and mitigation of photoelectric artifact simultaneously. The recording performance of Pt-PP coated optrode was investigated by CV, EIS and background noise tests in PBS solution. The results illustrated the outstanding recording performance of Pt-PP coating with lower impedance at 1 kHz and background noise (59 μV) than PEDOT/PSS and platinum black coating. Meanwhile, photoelectric artifact experiments *in-vitro* demonstrated the shortest recovery time of 0.3 ms and lowest artifact amplitude for Pt-PP coated optrode. *In-vivo* experiments proved higher SNR, lower artifact amplitude and shorter recovery time in the recording signals for Pt-PP coated optrode than platinum black coated one. Besides, the mechanical and electrochemical stability were verified by 100 min of ultrasonication and

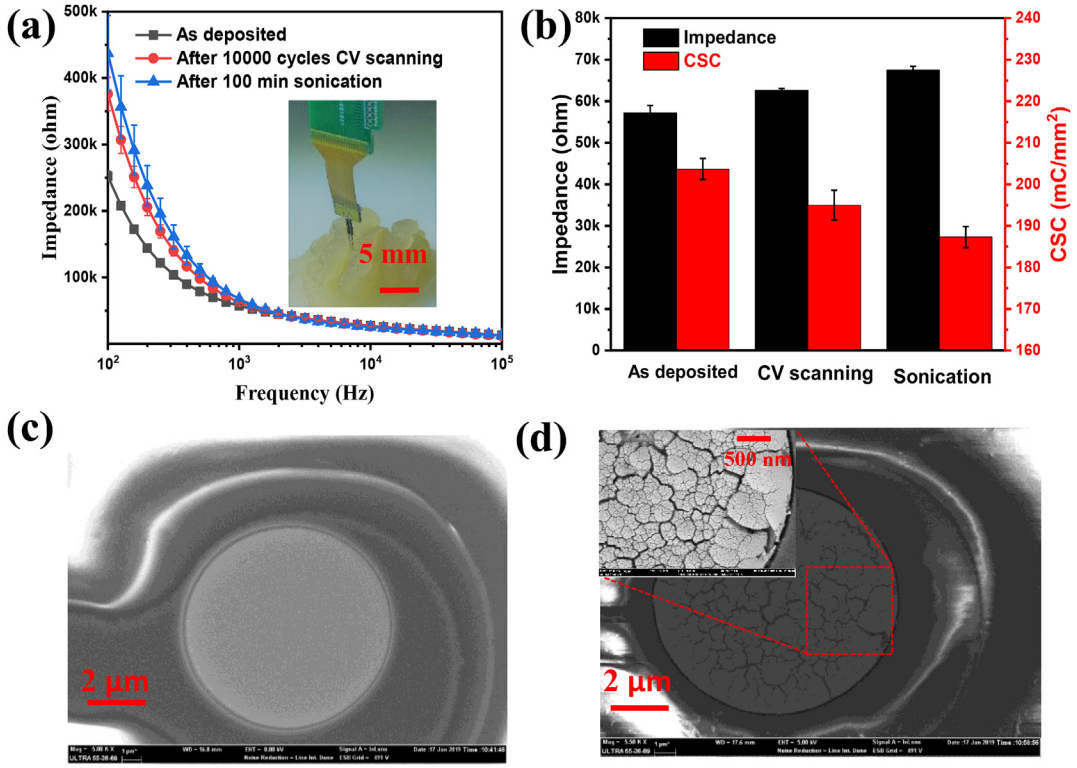

Fig. 4. (a) The impedance spectrum of the Pt-PP coated optrode after 0 cycle, 10000 cycles of CV scanning and 100 min ultrasonication (the inset showed the optrode was inserted into brain model made of agarose).(b) The histograms of CSC and impedance(at 1 kHz) variations with 10000 cycles of CV scanning and 100 min ultrasonication. (c) SEM image of the Bare Au electrode shows the smooth surface. (d) SEM images of the platinum black modified electrode, inset (Mag = 20.00K X) shows the rough and porous surface.

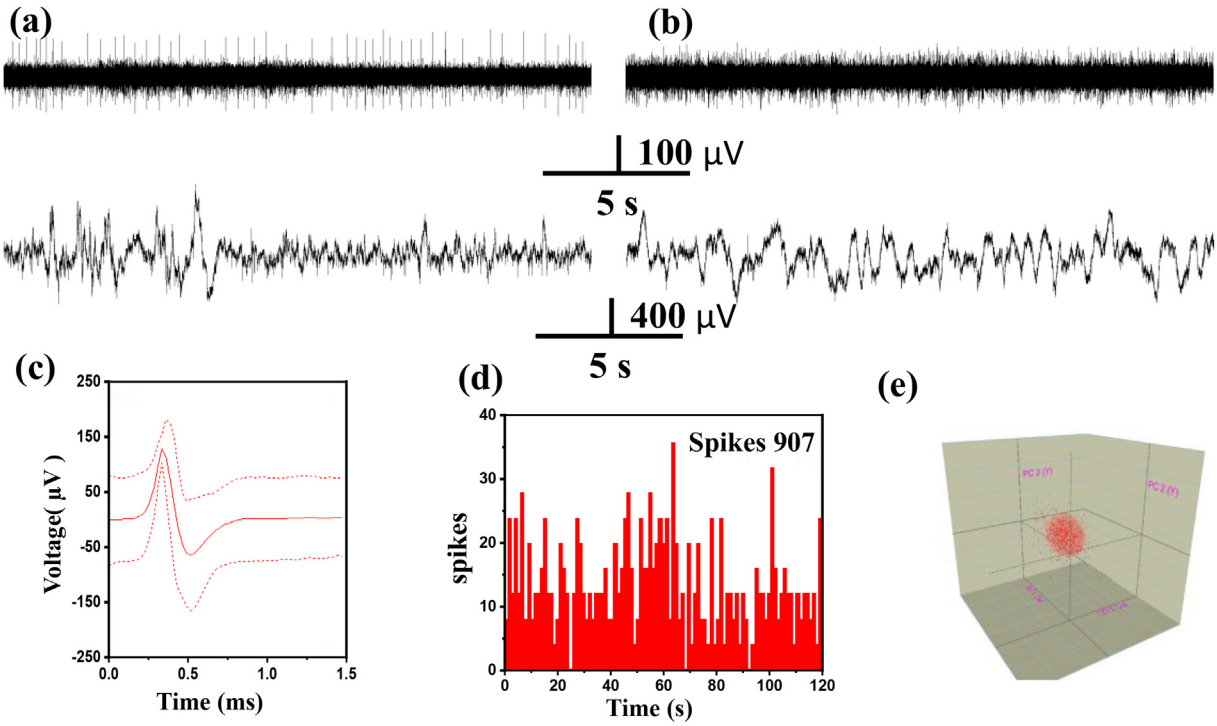

Fig. 5. The chronic recording results of Pt-PP coated and platinum black coated optrodes after four weeks of implantation. The spontaneous action potentials and local field potentials recorded from (a) Pt-PP modified electrode, (b) platinum black modified electrode. (c) The representative neural waveform with a peak-to-peak amplitude of 220 μV. (d) The firing events of neural during 120 s recording, (e) The PCA of sorted unit recorded from Pt-PP modified electrode.

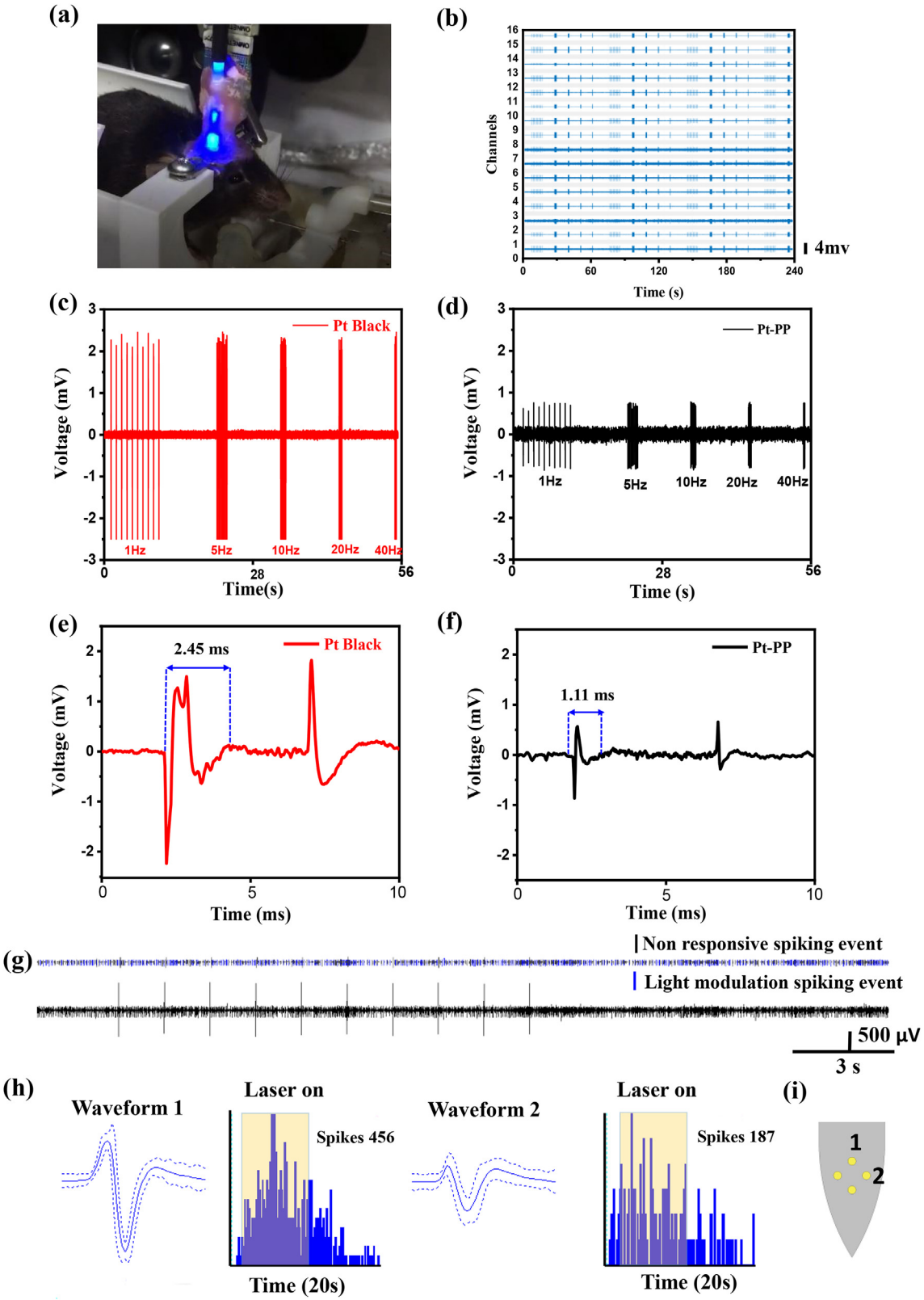

Fig. 6. The optogenetics experiments results *in-vivo*. (a) The photograph of a mouse implanted with Pt-PP coated optrode during photostimulation. (b) The spontaneous action potentials recorded from Pt-PP coated optrode. The recorded photoelectric artifact signal of (c) platinum black (d) Pt-PP coated optrode during photostimulation with a laser train (power of 2 mW, frequency of 1, 5, 10, 20, 40 Hz with 5 ms duration, 10 pulses for each frequency). The recorded artifact waveforms of (e) platinum black (f) Pt-PP coated optrode at laser power of 2 mW, frequency of 10 Hz, blue transverse line indicates the recovery time. (g) The raster pattern and recorded signal in one channel before and after applying a train of laser pulses (power of 2 mW, frequency of 10 Hz with 5 ms duration). (h) The waveforms and firing events of the same unit recorded from two different electrodes. (i) The relative position of two electrodes recording the same unit, and the unit is closer to electrode 1, demonstrates spatial resolution performance of Pt-PP modified optrode. (For interpretation of the references to colour in this figure legend, the reader is referred to the Web version of this article.)

10000 cycles of CV scanning tests. In short, the Pt-PP coating is an excellent candidate in the application of neural interface for the high SNR ensure the quality of recording signal and the lower artifact amplitude and shorter recovery time can greatly retain useful signals in optogenetics experiments. The shortcoming is the recording wires induced artifact can't be mitigate by Pt-PP coating, thus future work will focus on how to eliminate artifact by replacing electrode materials and make advance in probe structure to avoid direct light exposure of electrodes and recording wires.

CRediT authorship contribution statement

Long-Chun Wang: Conceptualization, Methodology, Validation, Writing - original draft. **Ming-Hao Wang:** Writing - review & editing, Validation. **Chao-Fan Ge:** Conceptualization, Methodology. **Bo-Wen Ji:** Writing - review & editing. **Zhe-Jun Guo:** Writing - review & editing. **Xiao-Lin Wang:** Writing - review & editing. **Bin Yang:** Writing - review & editing. **Cheng-Yu Li:** Supervision, Resources. **Jing-Quan Liu:** Funding acquisition, Writing - review & editing, Project administration.

Declaration of competing interest

The authors declare that they have no known competing financial interests or personal relationships that could have appeared to influence the work reported in this paper.

Acknowledgements

This work was partially funded by the National Key R&D Program of China under grant 2017YFB1002501, the National Natural Science Foundation of China (No. 61728402), the Research Program of Shanghai Science and Technology Committee (17JC1402800), the Program of Shanghai Academic/Technology Research Leader (18XD1401900). The authors are also grateful to the Center for Advanced Electronic Materials and Devices (AEMD) of Shanghai Jiao Tong University.

Appendix A. Supplementary data

Supplementary data to this article can be found online at https://doi.org/10.1016/j.bios.2019.111661.

References

Aleksandrova, E.L., 2007. Structural systematic features of photoelectric effect in aromatic polymers with polymethine dyes. Semiconductors 41 (12), 1445–1452.
Canales, A., Jia, X., Froriep, U.P., Koppes, R.A., Tringides, C.M., Selvidge, J., Lu, C., Hou, C., Wei, L., Fink, Y., Anikeeva, P., 2015. Multifunctional fibers for simultaneous optical, electrical and chemical interrogation of neural circuits in vivo. Nat. Biotechnol. 33 (3), 277–284.
Cardin, J.A., Carlen, M., Meletis, K., Knoblich, U., Zhang, F., Deisseroth, K., Tsai, L.H., Moore, C.I., 2009. Driving fast-spiking cells induces gamma rhythm and controls sensory responses. Nature 459 (7247), 663–667.
Cardin, J.A., Carlen, M., Meletis, K., Knoblich, U., Zhang, F., Deisseroth, K., Tsai, L.H., Moore, C.I., 2010. Targeted optogenetic stimulation and recording of neurons in vivo using cell-type-specific expression of Channelrhodopsin-2. Nat. Protoc. 5 (2), 247–254.
Cogan, S.F., 2008. Neural stimulation and recording electrodes. Annu. Rev. Biomed. Eng. 275–309.
Du, J., Roukes, M.L., Masmanidis, S.C., 2009. Dual-side and three-dimensional microelectrode arrays fabricated from ultra-thin silicon substrates. J. Micromech. Microeng. 19 (7), 075008.
Dufour, S., Lavertu, G., Dufour-Beausejour, S., Juneau-Fecteau, A., Calakos, N., Deschenes, M., Vallee, R., De Koninck, Y., 2013. A multimodal micro-optrode combining field and single unit recording, multispectral detection and photolabeling capabilities. PLoS One 8 (2), e57703.
Eshel, N., Bukwich, M., Rao, V., Hemmelder, V., Tian, J., Uchida, N., 2015. Arithmetic and local circuitry underlying dopamine prediction errors. Nature 525 (7568), 243–246.
Fekete, Z., 2015. Recent advances in silicon-based neural microelectrodes and microsystems: a review. Sens. Actuators B Chem. 215, 300–315.
Goncalves, S.B., Ribeiro, J.F., Silva, A.F., Costa, R.M., Correia, J.H., 2017. Design and manufacturing challenges of optogenetic neural interfaces: a review. J. Neural Eng. 14 (4), 041001.
Green, R.A., Lovell, N.H., Wallace, G.G., Poole-Warren, L.A., 2008. Conducting polymers for neural interfaces: challenges in developing an effective long-term implant. Biomaterials 29 (24–25), 3393–3399.
Han, X., Qian, X., Stern, P., Chuong, A.S., Boyden, E.S., 2009. Informational lesions: optical perturbation of spike timing and neural synchrony via microbial opsin gene fusions. Front. Mol. Neurosci. 2, 12.
Henriksen, B.S., Marc, R.E., Bernstein, P.S., 2014. Optogenetics for retinal disorders. J. Ophthalmic Vis. Res. 9 (3), 374–382.
Ji, B., Guo, Z., Wang, M., Yang, B., Wang, X., Li, W., Liu, J., 2018. Flexible polyimide-based hybrid opto-electric neural interface with 16 channels of micro-LEDs and electrodes. Microsys. Nanoengi. 4 (1).
Khurram, A., Seymour, J.P., 2013. Investigation of the photoelectrochemical effect in optoelectrodes and potential uses for implantable electrode characterization. Eng. Med. Biol. Soc., 6610179.
Kovalenko, I., Bucknall, D.G., Yushin, G., 2010. Detonation nanodiamond and onion-like-carbon-embedded polyaniline for supercapacitors. Adv. Funct. Mater. 20 (22), 3979–3986.
Kozai, T.D., Catt, K., Du, Z., Na, K., Srivannavit, O., Haque, R.U., Seymour, J., Wise, K.D., Yoon, E., Cui, X.T., 2016. Chronic in vivo evaluation of PEDOT/CNT for stable neural recordings. IEEE Trans. Biomed. Eng. 63 (1), 111–119.
Kravitz, A.V., Freeze, B.S., Parker, P.R., Kay, K., Thwin, M.T., Deisseroth, K., Kreitzer, A.C., 2010. Regulation of parkinsonian motor behaviours by optogenetic control of basal ganglia circuitry. Nature 466 (7306), 622–626.
LeChasseur, Y., Dufour, S., Lavertu, G., Bories, C., Deschenes, M., Vallee, R., De Koninck, Y., 2011. A microprobe for parallel optical and electrical recordings from single neurons in vivo. Nat. Methods 8 (4), 319–325.
Li, B., Lee, K., Masmanidis, S.C., Li, M., 2018. A nanofabricated optoelectronic probe for manipulating and recording neural dynamics. J. Neural Eng. 15 (4), 046008.
Lobo, M.K., Nestler, E.J., Covington 3rd, H.E., 2012. Potential utility of optogenetics in the study of depression. Biol. Psychiatry 71 (12), 1068–1074.
Ludwig, K.A., Uram, J.D., Yang, J., Martin, D.C., Kipke, D.R., 2006. Chronic neural recordings using silicon microelectrode arrays electrochemically deposited with a poly (3,4-ethylenedioxythiophene) (PEDOT) film. J. Neural Eng. 3 (1), 59–70.
Luo, Z., Qi, Q., Zhang, L., Zeng, R., Su, L., Tang, D., 2019. Branched polyethylenimine-modified upconversion nanohybrid-mediated photoelectrochemical immunoassay with synergistic effect of dual-purpose copper ions. Anal. Chem. 91 (6), 4149–4156.
Merrill, D.R., Bikson, M., Jefferys, J.G., 2005. Electrical stimulation of excitable tissue: design of efficacious and safe protocols. J. Neurosci. Methods 141 (2), 171–198.
Negi, S., Bhandari, R., Rieth, L., Solzbacher, F., 2010. In vitro comparison of sputtered iridium oxide and platinum-coated neural implantable microelectrode arrays. Biomed. Mater. 5 (1), 15007.
Petersen, H., Hagström, S.B.M., 1978. Optical excitation of the surface photoelectric effect of metals using synchrotron radiation. Phys. Rev. Lett. 41 (19), 1314–1317.
Royer, S., Zemelman, B.V., Barbic, M., Losonczy, A., Buzsaki, G., Magee, J.C., 2010. Multi-array silicon probes with integrated optical fibers: light-assisted perturbation and recording of local neural circuits in the behaving animal. Eur. J. Neurosci. 31 (12), 2279–2291.
Rui, Y.F., Liu, J.Q., Yang, B., Li, K.Y., Yang, C.S., 2012. Parylene-based implantable platinum-black coated wire microelectrode for orbicularis oculi muscle electrical stimulation. Biomed. Microdevices 14 (2), 367–373.
Seymour, J.P., Wu, F., Wise, K.D., Yoon, E., 2017. State-of-the-art MEMS and microsystem tools for brain research. Microsys. Nanoengi. 3, 16066.
Stark, E., Koos, T., Buzsaki, G., 2012. Diode probes for spatiotemporal optical control of multiple neurons in freely moving animals. Journal of neurophysiology 108 (1), 349–363.
Vazey, E.M., Aston-Jones, G., 2013. New tricks for old dogmas: optogenetic and designer receptor insights for Parkinson's disease. Brain Res. 1511, 153–163.
Wallden, L., 1985. Surface photoelectric effect for thin metal overlayers. Phys. Rev. Lett. 54 (9), 943–946.
Wang, M.-H., Ji, B.-W., Gu, X.-W., Guo, Z.-J., Wang, X.-L., Yang, B., Li, C.-Y., Liu, J.-Q., 2018a. A novel assembly method for 3-dimensional microelectrode array with micro-drive. Sens. Actuators B Chem. 264, 100–109.
Wang, M.H., Ji, B.W., Gu, X.W., Tian, H.C., Kang, X.Y., Yang, B., Wang, X.L., Chen, X., Li, C.Y., Liu, J.Q., 2018b. Direct electrodeposition of Graphene enhanced conductive polymer on microelectrode for biosensing application. Biosens. Bioelectron. 99, 99–107.
Weiland, J.D., Anderson, D.J., Humayun, M.S., 2002. In vitro electrical properties for iridium oxide versus titanium nitride stimulating electrodes. IEEE Trans. Biomed. Eng. 49 (12 Pt 2), 1574–1579.
Wu, F., Stark, E., Ku, P.C., Wise, K.D., Buzsaki, G., Yoon, E., 2015. Monolithically integrated muLEDs on silicon neural probes for high-resolution optogenetic studies in behaving animals. Neuron 88 (6), 1136–1148.
Zeng, R., Luo, Z., Su, L., Zhang, L., Tang, D., Niessner, R., Knopp, D., 2019. Palindromic molecular beacon based Z-scheme BiOCl-Au-CdS photoelectrochemical biodetection. Anal. Chem. 91 (3), 2447–2454.
Zhang, J., Zhao, X.S., 2012. Conducting polymers directly coated on reduced graphene oxide sheets as high-performance supercapacitor electrodes. J. Phys. Chem. C 116 (9), 5420–5426.